The effects of surface compliance on greyhound galloping dynamics

Journal Title
XX(X):2–24

DOI: 10.1177/ToBeAssigned
www.sagepub.com/
SAGE

Hasti Hayati[1] David Eager[1] and Paul Walker[1]

Abstract

Greyhounds are the fastest breed of dog and can reach a speed up to 68 km/h. These racing animals sustain unique injuries seldom seen in other breeds of dog. The highest rate of life-threatening injuries in these dogs is hock fracture, mostly of the right hind-leg. One of the main injury contributing factors in this sport is the track surface. There are some studies into the ideal track surface composition for greyhound racing but almost no study has investigated the body-surface interaction. Accordingly, the purpose of this work is to study the effect of surface compliance on the galloping dynamics of greyhounds during the hind-leg single-support phase which is a critical phase in hock injuries. Thus, a three degrees-of-freedom model for the greyhound body and substrate surface is designed using spring-loaded inverted pendulum method. The results showed that forces acting on the hind-leg were substantially affected when the surface compliance altered from the relatively hard (natural grass) to a relatively soft surface (synthetic rubber). The main contribution of this work is designing a mathematical model to predict the dynamics of the hock and the hind-leg as the most vulnerable body parts in greyhounds. Furthermore, this model can be used to optimise the greyhound track surface composition and therefore improve the safety and welfare within the greyhound racing industry.

Prepared using sagej.cls

Keywords

Greyhounds, hock injuries, SLIP model, galloping dynamics, foot-surface interaction

1 Nomenclature

g Gravitational acceleration

l Hind-leg length

$\dot{l}$ Hind-leg linear velocity

$\ddot{l}$ Hind-leg linear acceleration

m_b Overall mass of the greyhound

m_c Mass of the Clegg hammer

m_l Hind-leg mass of the greyhound

$[x]$ Vector of acceleration obtained from the accelerometers

$[\dot{x}]$ Vector of velocity obtained from the accelerometers

$[\ddot{x}]$ Vector of surface penetration obtained from the accelerometers

y Surface compression

$\dot{y}$ Surface linear velocity

$\ddot{y}$ Surface linear acceleration

C_s Surface damping coefficient

F Impact force of the Clegg hammer

K_l Hind-leg stiffness coefficient

K_s Surface stiffness coefficient

[1]School of Mechanical and Mechatronic Engineering, Faculty of Engineering and Information Technology, University of Technology Sydney, Ultimo, NSW, Australia

Corresponding author:
School of Mechanical and Mechatronic Engineering, Faculty of Engineering and Information Technology, University of Technology Sydney, Ultimo, NSW, Australia
Email: hasti.hayati@uts.edu.au

Prepared using sagej.cls *[Version: 2017/01/17 v1.20]*

T Kinetic energy

U Potential energy

$\mathcal{L}$ Lagrangian

θ Hind-leg angle with respect to the ground

$\dot{\theta}$ Hind-leg angular velocity

$\ddot{\theta}$ Hind-leg angular acceleration

2 Introduction

Greyhounds are a breed of dog that belongs to the family of sight hounds. The sight hounds' ability to sprint and chase prey has made them a reliable food hunting assistant throughout history[1]. The greyhound has a maximum speed in excess of 65 km/h[2]. The rotary gallop is the greyhounds' preferred galloping gait. It is their fastest gait but the most fatiguing one[3]. Greyhound racing tracks vary in shape and design and can either have sand or natural grass surface. Races are run anti-clockwise with usually six to eight greyhounds in each race.

The kinetics and kinematics of greyhound's gaits have been analysed in the literature. In a study conducted by Marghitu and Nalluri[4], 2-dimensional motion measurement and analysis system (Peak Performance Technologies, Inc. Englewood CO) was used to compare the hind-legs trajectories of three healthy greyhounds with those with tibial nerve paralysis. It is proved that their method could successfully distinguish healthy and unhealthy cases. In another kinematic study on greyhounds conducted by Owen et al.[5], the familiarisation-time required for greyhounds to have a reliable trotting gait on a treadmill was studied. Hudson et al.[6] also investigated the reasons lies behind the considerable maximum speed difference between greyhounds and cheetahs. It is found that the longer stride-length/lower stride frequency adapted by cheetah is the main reason for their higher top speed than a greyhound.

Greyhounds sustain unique types of injuries that are rarely seen in other breeds of dogs[7]. The injuries are mostly musculoskeletal injuries that are involved in locomotion and rapid acceleration[8]. Hip and hock joints of the right hind-leg, which is usually the leading limb in greyhounds, were proven to play a

significant role in powering the locomotion[9]. Furthermore, the hock joint also withstands the initial force due to impact with the ground. Thus, it is not unexpected that hock fracture of the right hind-leg is among the most common career-ending injuries in the greyhounds[10,11].

The race track surface is believed to be one of the main factors contributing to injury.[12–16]. The ideal track surface should act to absorb the impact forces of the foot, provide traction for a controlled gallop and efficient use of energy[17]. Any inconsistency on the track surface is dangerous and can cause an injury[2,17] as the greyhound is not capable of adjusting its gait based on changing surface conditions[18]. Although there are researches on the surface composition of race tracks, there is still a big gap in investigating the interaction of race track surface with greyhound sprinting[8,13].

McMahon et al.[19] were among the pioneers that looked into the impact of surface compliance on running dynamics. They designed a two degrees-of-freedom (DOF) spring-mass model representing the legs and track surface. The objective was to predict the effect of surface compliance on step length and ground contact time. A single lane running surface with a 26.25 m length, made of plywood boards (40.6 cm $\times$ 121.9 cm $\times$1.5 cm) was designed to verify the model. The plywood boards were screwed to 4.4 cm $\times$ 8.9 cm and served as supports. Moving the supporting rails could alter the spring coefficient of the surface. A Kistler force plate (model 9261A) was mounted beneath the track to measure the foot force. Eight healthy male subjects ran over the experimental wooden track. Analysing the foot force result on a hard surface showed a spike five times the average body weight of the runners, which disappeared on a very compliant surface. However, running on a compliant surface with the stiffness 0.15 times of man's body stiffness, reduced the speed up to 0.7 times compared to a hard surface. Finally, a moderately compliant surface, which is found to have a stiffness three times of man's body stiffness, increased the speed up to 2% and correlated to low injury rate.

Inertial measurement units (IMU), are also used to study the impact of the substrate surface on the locomotion dynamics of animals of different sizes and species. Spence et al.[20] designed an accelerometer backpack to study the dynamics of an insect (adult Death's head cockroaches) Centre of Mass (CoM) when running on compliant surfaces. The results showed smaller spikes in vertical acceleration when

an insect ran on elastic surfaces. Moreover, in the recent work conducted by Hayati et al., an in-house IMU was used to measure the acceleration upon galloping in racing greyhounds. A greyhounds was encouraged to run on two tracks with different surface materials (natural grass and sand) and lower peaks in forward acceleration on softer (grass surface) than harder one (sandy surface) were observed[21]. Using a theodolite and high frame rate (HFR) videos to match paw prints with acceleration signals, it was shown that the spikes in the signals (both forward and vertical accelerations) were due to hind-leg impacts on the ground[22–24].

Apart from experimental methods used to study the surface impacts on locomotion dynamics, the Spring Loaded Inverted Pendulum (SLIP) model is the simplest and the most extensively used way addressing legged locomotion in humans, animals and robots. It consists of a mass, located at the CoM of the system and usually massless compliant legs[25–27].

Gayer et al. showed that, owing to the behavior of compliant legs, a simple bipedal SLIP model is capable of simulating different varieties of gaits[26]. Moreover, SLIP models are also capable of explaining the dynamics of legged motion both during stance and flight (when no legs are on the ground). For instance, recently the SLIP model was used to explain swing leg kinetics during the human walking gait[28].

In this work, the effect of surface compliance on galloping greyhounds' hind-leg dynamics is studied. It is observed that the force acting on the hind-leg was affected (13% increase) when the surface compliance altered from a relatively soft to a relatively hard surface. Moreover, the force acting on the hind-leg was almost nine times the force acting on the CoM. Accordingly, this study provides an invaluable basis for further work on designing safe race track surfaces.

3 Methods

3.1 Kinematic Analysis

Four greyhounds were encouraged to run at a track with a natural grass surface (Cessnock Track, NSW, Australia) during a trial session. Greyhounds were released from 'Starting boxes' located at the 400 m race distance and started to chase a mechanical lure driven by a lure driver. The 400 m race started inside the turn, followed by a long straight section, called the 'Home straight', then the 'Finish line' and finished at the 'Catching pen' where greyhounds were collected by the owners.

A Sony DSC-RX10-III camera (adjusted to 500 frame per seconds) was mounted on a tripod outside the track, behind the outer rails and captured greyhounds from a Sagital view. The camera location was almost at the end of the Home straight to allow enough time for greyhounds to achieve a steady-state gallop. Using the recorded HFR videos, the footfall timing of greyhounds' rotary gallop in a single stride were calculated and their hip joint during the hind-leg single support phase were tracked.

3.1.1 Rotary galloping and Footfall Timing Gait refers to a pattern of limb actions that an animal uses repetitively during locomotion. There are two types of galloping gait: the transverse gallop and the rotary gallop. The transverse gallop is usually seen in horses whereas the rotary gallop is used by cheetahs and greyhounds[29].

The rotary gallop is a four-beat gait with two flight phases. Based on the observations most of the greyhounds were 'left-pawed' with an anti-clockwise pattern of paw impacts (Fig. 1.B). The pattern of limb impacts in this gait is rotating i.e. left fore-leg (LF), right fore-leg (RF), compressed flight phase (CFL), right hind-leg (RH), left hind-leg (LH) and extended flight phase (EFL) (Fig. 1.B and C).

The Hind-leg stance consists of three different phases: the first single-support phase (which is usually the RH), a double-support phase when both hind-legs are on the ground, and the second single-support phase (which is usually the LH). HFR analysis of greyhounds galloping showed less than 10 ms seconds overlap between RH and LH in the double-support phase. However in this paper, only the hind-leg "first"

single-support phase and its interaction with the surface is considered. For the sake of simplicity and readability of the article, this phase is referred to as as 'RH single-support' hereinafter.

Footfall timing and duty factor (the ratio of limb's stance and total stride duration) of each limb, namely LF, RF, CFL, RH, LH and EFL, were measured and tabulated in Table 1.

Table 1. Average of stance and flight duration and limb duty factor of galloping greyhounds.

Stride events	Duration (ms)	Duty factor (β)
LF	52.7, SD= 5.1	0.169
RF	58.1, SD= 6	0.188
CFL	58.6, SD= 5.3	-
RH	52.5, SD= 4.13	0.169
LH	64.7, SD= 6.6	0.208
EFL	63.5, SD= 9.8	-

3.1.2 The Hip joint and CoM tracking during hind-leg single support phase HFR videos of four greyhounds galloping in the Home straight of a race track with natural grass surface (Cessnock track, NSW, Australia) were captured by Sony DSC-RX10-III in 500 frame per seconds. The videos were then post-processed using Kinovea (version 08.26) which has previously been reported in the literature[30,31]. A reference pole with a length of 500 mm was attached to the inner rail of the race track to calibrate the video.

Animal ethics approval was obtained (UTS ACEC ETH160367). This placed several restrictions on the testing including use of sensors and adhesives for attaching "markers". No adverse effects on animal behavior due to filming the greyhounds were observed. Owing to the animal ethics agreement, this required a good deal of manual tracking of greyhound hip joint and CoM (lies 60% along the way from hip to shoulder joints[32]), during hind-leg single support to generate the results provided in this paper. The following steps were manually adapted for motion tracking:

- Specify the touch down of RH single-support (Fig. 2. A) and set it as the coordinate reference point.

- Draw a reference line from the approximate location of the hip joint and shoulder joint. Estimate the CoM location (60% along the way from hip to shoulder joints[32]) on the reference line (Fig. 2. B).
- Track greyhounds' hip joint and CoM during RH single-support using Kinovea semi-automatic tracking toolbox. Only the hind-leg compression vs time during RH single-support is illustrated (Fig. 2. C).

The results of this section were used to validate the simulations explained in the following sections.

3.2 SLIP modelling

The purpose of this paper was to study the interaction of greyhound RH single-support and track surface, as the right hind-leg has shown to have a considerable rate of injuries[10,11,33]. To do the SLIP method was used which has been shown to be successful in explaining the legged locomotion. In the simplest SLIP models , the overall mass of the object is usually lumped on the CoM with massless linear springs, representing the legs[26].

Accordingly, in the first attempt, the greyhound and the surface was modelled as a 4 DOF system which is shown in Fig. 3.A. The body is modelled as a rigid beam with the mass of m_b. The legs are modelled as linear springs. During RH single-support, mass of the hind-legs (m_l) was assumed to be concentrated on the toe. Leg compression (l), surface compression (y), leg rotation (θ_1) and body tilting (θ_2) were the independent degrees of freedom of the system.

However, a closer look at the HFR videos of greyhounds during RH single-support indicated that the ratio of body tilting and leg rotation was negligible or in other words the body hardly tilted during this phase. Accordingly, the model was simplified which is shown in Fig 3.B. This made the model a 3 DOF system where the body mass was lumped on the hip joint. The contact between the hind-legs (the linear spring) and the surface is modeled as frictionless pin joint. The same simplified model was shown to be accurate enough by Gayer et al. in simulating running and walking gaits[26].

The 3 DOF system is consisted of the leg compression (l), leg rotation (θ), and surface compression (y). Lagrange method is deployed to obtain the system equation of motion (EOM) (Equation 1 to 4).

$$T = \frac{1}{2}m_b\dot{l}^2 + \frac{1}{2}m_b l^2\dot{\theta}^2 + \frac{1}{2}m_l\dot{y}^2 \tag{1}$$

$$U = \frac{1}{2}K_l(l-y)^2 + \frac{1}{2}K_s y^2 + m_b g l sin(\theta) \tag{2}$$

$$\mathcal{L} = T - U \tag{3}$$

$$\frac{d}{dt}\left(\frac{\sigma\mathcal{L}}{\sigma\dot{q}}\right) - \frac{\sigma\mathcal{L}}{\sigma q} \tag{4}$$

where T is the Kinetic energy, U is the Potential energy, and $\mathcal{L}$ is the Lagrangian. The state variables are shown as $q = [l, \theta, y]^T$ and $\dot{q} = [\dot{l}, \dot{\theta}, \dot{y}]^T$. The EOM is given in the Equations 5 to 7.

$$m_b\ddot{l} + K_l(l-y) + C_s\dot{x} - 2m_b l\dot{\theta}^2 - m_b g sin(\theta) = 0 \tag{5}$$

$$2m_b l^2\ddot{\theta} + 4m_b l\dot{l}\dot{\theta} + m_b g l cos(\theta) = 0 \tag{6}$$

$$m_l\ddot{y} + K_l(y-l) + K_s(y) + C_s\dot{y} = 0 \tag{7}$$

where m_b represents greyhound's overall mass, m_l represents hind-leg mass, K_l represents hind-leg stiffness coefficient, K_s represents surface stiffness coefficient, C_s represents surface damping coefficient, l represents the hind-leg length, $\dot{l}$ represent the hind-leg linear velocity, $\ddot{l}$ represent the hind-leg linear acceleration, y represents surface compression, $\dot{y}$ represents surface linear velocity, $\ddot{y}$ represents surface linear acceleration, θ represents hind-leg angle, $\dot{\theta}$ represents leg angular velocity, and $\ddot{\theta}$ represents leg angular acceleration.

3.3 Surface stiffness and damping coefficient

In order to obtain the surface stiffness (K_s) and damping (C_s) coefficient, which was required as the input of the SLIP model, an impact test using an in-house modified Clegg impact hammer (the Clegg hereinafter) was conducted. The Clegg was developed by Branden Clegg to control the compaction of road materials[34]. The apparatus consists of a guided tube and a flattened cylindrical mass. The mass is located inside the tube and should be dropped at standard height on the surface. The Clegg measures the peaks of deceleration when the mass comes into contact with the surface in the units of ten of gravity[34,35].

However, in order to obtain the stiffness coefficient of the surface, a line should be fitted on the loading phase of the load-deformation plots. This procedure was used in obtaining the stiffness coefficient of athletic shoes[36] and is explained in detail in the following sections. Accordingly, the Clegg was modified by adding two identical high-g (500 g) piezo-resistive accelerometers (Endevco-7264B-500T). The Clegg and the accelerometers together weighed 2.28 kg. The surface area of the Clegg circular contact surface was 19.63 cm^2 (i.e. 50 mm diameter). The software was written in LabVIEW. The accuracy of the software to process the acceleration data has been proven in the literature[37,38]. The data acquisition unit had the sampling rate of 25000 Hz and complied with AS 4422 standard[39]. A low-pass filter of channel frequency class of 1000 was used.

The Clegg was dropped three times from different heights (400, 500 and 600 mm) on two different surfaces: natural grass and synthetic rubber. Testing on rubber surface was conducted in the lab environment whereas testing on natural grass was conducted in-situ (Cessnock greyhound racing track, NSW, Australia). Impacts were carried out on different locations of surface to avoid surface compression that could affect the impact data. The impact data were then post-processed using LabVIEW software and plotted in MATLAB R18.

Hysteresis was seen in the plots given in Fig. 4 which revealed the viscoelastic properties in both the rubber and natural grass surface. As the loading parts of the plots for subsequent impact velocities coincided, to get the effective spring coefficient, the slope of the linear phase of 3.4 m/s impact velocity

(indicated by the dashed lines), was calculated. The effective spring coefficient equaled 107 kN/m and 68.2 kN/m for natural grass and synthetic rubber, respectively.

The area inside the hysteresis loops is the energy loss of the surfaces. The average of energy loss from three different heights was calculated for both surfaces and equaled to 9.87 J and 5.45 J for grass and rubber, respectively. To get the damping coefficient, the following equation was considered:

$$F = m_c[\ddot{x}] + c_s[\dot{x}] + k_s[x] \tag{8}$$

where F is the force of the Clegg when impacting the ground from different heights, m_c=2.28 kg is the mass of the Clegg and accelerometers, $[\ddot{x}]$ is the vector of acceleration data obtained from the accelerometers, $[\dot{x}]$ is the vector of velocity integrated from the acceleration data, and $[x]$ is the surface penetration obtained from integrating velocity data. The only unknown in Equations. 8 is the damping coefficient which can be determined by the nonlinear least squares method. Using the MATLAB "*lsqnonlin* function", the damping coefficient was calculated and equaled to 89.6 N.s/m and 81.4 N.s/m for natural grass and synthetic rubber, respectively. However, it should be mentioned that the damping coefficient depends on different variables such as, temperature, impact velocity, acceleration, shape, and type of stress (compression, tensile, or shear), so the obtained values may alter depending on the loading conditions.

Accordingly, all the required inputs for the 3 DOF SLIP model were obtained which are tabulated in the Table 2 below:

Using the initial conditions tabulated in Table 2, the Runge Kutta method was deployed to solve the nonlinear second order differential equations using ode45 solver in MATLAB R18.

Table 2. Initial conditions for galloping gait.

Parameters	Determination	Value
m_b	Jayes et al. study[40]	32 kg
m_l	Jayes et al. study[40]	3.4 kg
k_l	Farley et al. study[41]	From 4.24 kN/m to 4.92 kN/m
k_s	Clegg Hammer Experiment	68.2 kN/m and 107 kN/m
c_s	Clegg Hammer Experiment	89.6 N.s/m and 81.4 N.s/m
l_0	Measured form the HFR videos	From 700 mm to 900 mm
$\dot{l_0}$	Estimated from the HFR videos	From 11.3 m/s to 12.5 m/s
θ	Estimated from the HFR videos	From 2.28 rad to 2.39 rad
$\dot{\theta_0}$	Estimated from the HFR videos	From 11 rad/s to 13 rad/s
y	-	0 mm
$\dot{y_0}$	Approximated	From 11.3 m/s to 12.5 m/s

4 Results and Discussion

In this section, firstly the simulation results were verified with the experimental data which was explained earlier in the kinematic analysis section. Secondly, the simulation results, namely the hind-leg compression vs time, hind-leg rotation vs time, surface compression vs time, CoM trajectories, force applied on the CoM vs time (hereinafter GRF) and force applied on the hind-leg vs time (hereinafter Impact Force) for natural grass and synthetic rubber surfaces, during RH single-support in all the aforementioned cases were plotted and analysed.

4.1 Simulation verification

To verify the 3 DOF SLIP model, the hind-leg compression (Fig. 5.A) and rotation (Fig. 5.B) of four galloping greyhounds during RH single-support on the natural grass surface are compared, with the simulation results. The initial conditions in the model were changed as per the experimental data to achieve the best fit.

The simulation results are shown as rigid lines and the experimental data are shown as scattered dots. The model inputs (l, θ, $\dot{l}$, $\dot{\theta}$) in 3 DOF system were changed based on the experimental data. Thus, the same colours in the scattered dots correspond to the model with similar initial conditions e.g. red scattered plot corresponds to red simulated results.

Root Mean Square Error (RMSE) between the model and data was 1.59 mm for hind-leg compression and 0.23 rad for hind-leg rotation vs time. The reported RMSE values here were the average of four conditions. This suggests a good agreement between simulated results and experimental data as it was able to qualitatively and quantitatively predict greyhound's RH single-support dynamics.

4.2 Effect of surface compliance on RH single-support dynamics

Dynamics of greyhound RH single-support (Hind-leg compression, hind-leg rotation, surface compression, hip joint trajectories, GRF and Impact Force) are compared in two different surface conditions and illustrated in Fig.6. The black rigid lines and blue dashed lines illustrate the natural grass and synthetic rubber surfaces respectively. To achieve the highest possible accuracy, the initial conditions with the highest corroboration with the experimental data were used.

Hind-leg compression versus time, during RH single-support, is depicted in Fig. 6.A. The motion starts from the extended length of the hind-leg (781 mm), reaches its minimum length in the middle of the RH single-support (mid-stance hereinafter) and starts expanding afterward. The model predicts the RH single-support duration with less than 20% error (53.5 ms vs 52.5 ms). As can be seen the limb does not reach its initial length in this cycle. The consecutive dynamic after RH single-support is RH double-support which allows enough time for the leg to extend and finally lift-off from the ground. This dynamic is not considered in this study. Moreover, the results of the models with natural grass and with rubber are similar and the plots are almost superimposed on each other. This suggests that the current surface compliance does not have considerable impacts on overall hind-leg compression during RH single-support.

Hind-leg rotation vs time, during RH single-support, is depicted in Fig. 6.B. The initial angle of the leg with respect to the ground is 2.269 rad. During mid-stance the leg is perpendicular with the ground. At the end of the motion, the hind-leg angle is 1.014 rad. Similar to hind-leg compression vs time, surface compliance does not have any effect on the hind-leg rotation and is similar in both surface conditions

Surface compression vs time, during RH single-support is shown in Fig. 6.C. The grass surface has lower frequency but higher amplitude whereas the rubber surface has higher frequency but lower amplitude. At first both surfaces are compressed to roughly to 25.3 mm. However, they diverge eventually due to their different natural frequency. As discussed above, the surface compliance did not have any considerable impacts on the overall hind-leg compression (Fig. 6.A).

CoM trajectories during RH single-support are depicted in Fig. 6.D. In the model these data were extracted from the combination of both hind-leg compression and and rotation information generated by the model. No difference was seen between trajectories of the CoM on different surface compliance.

In order to calculate the GRF during RH single-support, the absolute value of hind-leg compression (l) generated by the model is used which is then multiplied by the spring coefficient of the leg (K_l). The leg spring coefficient was obtained from Farley et al. study[41] where the leg spring coefficient for different animals of different sizes were measured.

It was found that the leg stiffness (k_{LEG}) only slightly increased with forward speed for all animals or in other words it was independent of the speed. Moreover, the k_{LEG} value of a dog with the average mass and length of 23 kg and 0.5 m, was determined to be equal to 4.24 to 4.92 kN/m[41]. It is worth noting that the reported value K_l is not specific to greyhounds, nevertheless, it was the closest value for our study.

Accordingly, GRF during RH single-support is illustrated in Fig. 6.E. The results of this study are compared with the Williams et al. study[9]. The objective was to study the biomechanical strategies enabling greyhounds to achieve an effective acceleration during galloping. To do so, the simultaneous kinematic and kinetic analysis through HFR videos of speed cameras (ProReflex, Qualisys, Gothenburg, Sweden) and GRF data of force platforms (AMTI, Watertown, MA, USA) were collected, respectively. Eleven greyhounds were analysed in total with low (acceleration ranging from 0.5 to 1.2 m/s^2) and high (acceleration ranging from 2.8 to 4.4 m/s^2) accelerations. It was found that the greatest increase in joint work and power with acceleration appeared to be at the hip and hock joints. Moreover, the largest increase in absolute positive joint work appeared at the hip joint, supporting the fact that quadrupeds power locomotion by torque about their hip joint. The measured GRF of the leading hind-leg with low

and high acceleration were roughly 1.2 and 1.6 times of the average body weight of a greyhound. The current model in this work has predicted this to be 2.5 times the greyhound's body weight (810 N) which seems consistent considering the following limitation.

Firstly, in the current model the greyhound during a steady-state gallop is considered which means the animal was galloping with a constant speed. Secondly, this model was a simplified version of greyhound anatomical structure. The sophisticated structure of the hind-leg was modeled with a linear spring and a concentrated mass on the toes, and the rest of the body was modeled with a lumped mass on the hip joint.

The Impact Force during RH single-support is calculated by multiplying the surface compression (y) by the surface stiffness coefficient (K_s) which is depicted in Fig. 6.F. According to "Newton's third law" the same amount of the load but in the opposite direction, acts on the hind-leg from the surface.

The Impact Forces of both surfaces were seen to have three peaks during RH single-support. In both cases the second peak had the highest value. On natural grass surface the values for the first to the third peaks were 2600 N, 7200 N and 2400 N, respectively. On the synthetic rubber surface the values for the first to the third peaks were 1800 N, 6200 N and 1300 N, respectively. In addition, comparing the Impact Force and GRF, the Impact Force in natural grass was more than eight times higher than the GRF. The Impact Force in synthetic rubber was seven times higher than the GRF.

In a recent study by Hayati et al. conducted on thirteen tracks in NSW, Australia, 74% of catastrophic injuries were on the hind-leg with 52% of them on the right hock. The injury mechanism was not analysed in this study [10].

Moreover, in a study conducted by Bloomberg et al. [33], it was mentioned that there was a tendency in tarsal injuries to increase in each successive race which was believed to be due to the disturbance of the surface from previous race. This suggests that tarsal dynamics are affected by surface compliance which is in agreement with our results (high amount of force is acting on the hind-leg during each limb strike). In each successive race, as greyhounds are racing, the track becomes more compacted and therefore harder. This is in agreement with our model data that as the harder surface had higher Impact Force.

In addition, in a study done by Hayati et al. a tri-axial accelerations upon galloping in racing greyhounds were measured via an IMU embedded in a pocket sewn into a greyhound racing jacket[22]. It was found that the spikes appearing in forward and vertical accelerations were due to hind-leg strikes. This suggested high loads were acting upon each leg strike which was also predicted by the current 3 DOF SLIP model.

5 Conclusion

The purpose of this work was to study the effect of surface compliance on the locomotion dynamics of racing greyhounds, during the most critical phase of the galloping gait, RH single-support. To do so, a 3 DOF model of greyhound's body and underneath surface was designed using SLIP method. The results showed that the forces acting on the hind-leg were substantially affected when the surface compliance altered from the relatively hard (natural grass of the typical race track with a stiffness coefficient of k=107 kN/m) to a relatively soft surface (synthetic rubber with a stiffness coefficient of k=68.2 kN/m). The forces acting on the hind-leg were almost nine times the forces acting on the dog's centre of mass for natural grass surfaces (7200 N vs 810 N) which was in agreement with the high rate of hock fracture stated in the literature. The model was verified with experimental data of the hip trajectories of four healthy greyhounds galloping over a natural grass surface. To conclude, this simple SLIP model was able to predict the dynamics of greyhounds' galloping gait on surfaces of different compliance, during the hind-leg single support phase. The model also highlighted the importance of surface compliance and its influence on an elevated risk of hock injuries in racing greyhounds. In future, the effect of surface compliance on RH double-support to explain the considerable difference in injury data between the leading and trailing hind-leg in racing greyhounds will be studied.

Acknowledgements

Thanks go to Mr Chris Chapman, Manager, UTS Dynamic and Mechanics of Solids Laboratory, for assisting with instrumentation associated with the Clegg Hammer test. The authors would also like to thank Greyhound Racing NSW for funding this project.

References

1. Cunliffe J. *Sight Hounds: Their History, Management and Care*. Swan Hill Press, 2006. ISBN 1904057780.
2. Davis PE. Toe and muscle injuries of the racing greyhound. *New Zealand Veterinary Journal* 1973; 21(7): 133–146. DOI:10.1080/00480169.1973.34094. URL http://dx.doi.org/10.1080/00480169.1973.34094.
3. Biewener AA. *Animal locomotion*. Oxford University Press, 2003. ISBN 019850022X.
4. Marghitu DB and Nalluri P. An analysis of greyhound gait using wavelets. *Journal of Electromyography and Kinesiology* 1997; 7(3): 203–212.
5. Owen M, Richards J, Clements D et al. Kinematics of the elbow and stifle joints in greyhounds during treadmill trotting an investigation of familiarisation. *Veterinary and Comparative Orthopaedics and Traumatology* 2004; 17(03): 141–145.
6. Hudson PE, Corr SA and Wilson AM. High speed galloping in the cheetah (acinonyx jubatus) and the racing greyhound (canis familiaris): spatio-temporal and kinetic characteristics. *Journal of Experimental Biology* 2012; 215(14): 2425–2434.
7. Hickman J. Greyhound injuries. *Journal of Small Animal Practice* 1975; 16(12): 455–460.
8. Beer LM. *A study of injuries in Victorian racing greyhounds 2006-2011*. Master thesis, The University of Melbourne, 2014.
9. Williams SB, Usherwood JR, Jespers K et al. Exploring the mechanical basis for acceleration: pelvic limb locomotor function during accelerations in racing greyhounds (canis familiaris). *The Journal of Experimental Biology* 2009; 212(4): 550–565.

10. Hayati H, Eager D, Stephenson R et al. The impact of track related parameters on catastrophic injury rate of racing greyhounds. In *9th Australasian Congress on Applied Mechanics (ACAM9) 2017*. Engineers Australia, p. 311.
11. Jones J. *Repair of hock fractures in racing greyhounds*. British Medical Journal Publishing Group, 2009.
12. Angle T, Gillette RL and Weimar WH. Caudal paw displacement during movement initiation and its implications for possible injury mechanisms. *Veterinary and Comparative Orthopaedics and Traumatology* 2012; 25(5): 397–401.
13. Cook A. Literature survey of racing greyhound injuries, performance and track conditions. *Journal of Turfgrass Science* 1998; 74: 108–113.
14. Davis P. Track injuries in racing greyhounds. *Australian veterinary journal* 1967; 43(5): 180–191.
15. Iddon J. The effect of season and track condition on injury rate in racing greyhounds. *Journal of Small Animal Practice* 2014; 55(8): 399–404.
16. Prole J. A survey of racing injuries in the greyhound. *Journal of Small Animal Practice* 1976; 17(4): 207–218.
17. Gillette L. Optimizing performance and prevent injuries of the canine sprint athlete. In *North American Veterinary Conference 2007*.
18. Gillette L. Track surface influences on the racing greyhound. *Greyhound review* 1992; 20: 41–44.
19. McMahon TA and Greene PR. The influence of track compliance on running. *Journal of biomechanics* 1979; 12(12): 893–904.
20. Spence AJ, Revzen S, Seipel J et al. Insects running on elastic surfaces. *Journal of Experimental Biology* 2010; 213(11): 1907–1920.
21. Hayati H, Walker P, Mahdavi F et al. A comparative study of rapid quadrupedal sprinting and turning dynamics on different terrains and conditions: racing greyhounds galloping dynamics. In *ASME 2018 International Mechanical Engineering Congress and Exposition*. American Society of Mechanical Engineers, pp. V04AT06A047–V04AT06A047.
22. Hayati H, Eager D, Jusufi A et al. A study of rapid tetrapod running and turning dynamics utilizing inertial measurement units in greyhound sprinting. In *ASME 2017 International Design Engineering Technical*

Conferences and Computers and Information in Engineering Conference. American Society of Mechanical Engineers, pp. V003T13A006–V003T13A006.

23. Hayati H, Eager D, Brown T et al. Stride length as a speed indicator in fast quadrupeds. In *International Society of Biomechanics (ISB 2017)*.
24. Hayati H, Eager D, Jusufi A et al. A novel approach to analyzing rapid tetrapod locomotion using inertial measurement units. In *International Society of Biomechanics (ISB 2017)*.
25. Blickhan R and Full R. Similarity in multilegged locomotion: bouncing like a monopode. *Journal of Comparative Physiology A: Neuroethology, Sensory, Neural, and Behavioral Physiology* 1993; 173(5): 509–517.
26. Geyer H, Seyfarth A and Blickhan R. Compliant leg behaviour explains basic dynamics of walking and running. *Proceedings of the Royal Society of London B: Biological Sciences* 2006; 273(1603): 2861–2867.
27. Holmes P, Full RJ, Koditschek D et al. The dynamics of legged locomotion: Models, analyses, and challenges. *Siam Review* 2006; 48(2): 207–304.
28. Song H, Park H and Park S. A springy pendulum could describe the swing leg kinetics of human walking. *Journal of Biomechanics* 2016; 49(9): 1504–1509. DOI:https://doi.org/10.1016/j.jbiomech.2016.03.018. URL http://www.sciencedirect.com/science/article/pii/S0021929016303098.
29. Hildebrand M. The adaptive significance of tetrapod gait selection. *American Zoologist* 1980; 20(1): 255–267.
30. Baude M, Hutin E and Gracies JM. A bidimensional system of facial movement analysis conception and reliability in adults. *BioMed research international* 2015; 2015: 1–8.
31. Damsted C, Nielsen RO and Larsen LH. Reliability of video-based quantification of the knee-and hip angle at foot strike during running. *International journal of sports physical therapy* 2015; 10(2): 147–154.
32. Bertram JE. *Understanding mammalian locomotion: concepts and applications*. John Wiley & Sons, 2016. ISBN 0470454644.
33. Bloomberg M. Racing greyhound track injuries. In *Annual International Racing Greyhound Symposium Florida 1989*. pp. 3–12.

34. Clegg B. An impact testing device for in situ base course evaluation. In *Australian Road Research Board Conference Proceedings 1976*, volume 8.

35. Mohajerani A, Kurmus H, Tran L et al. Clegg impact hammer: an equipment for evaluation of the strength characteristics of pavement materials, turf, and natural and artificial playing surfaces: a review. *Journal of Road Materials Pavement Design* 2018; : 1–19.

36. Aerts P and Clercq DD. Deformation characteristics of the heel region of the shod foot during a simulated heel strike: the effect of varying midsole hardness. *Journal of sports sciences* 1993; 11(5): 449–461.

37. Eager D and Hayati H. Additional injury prevention criteria for impact attenuation surfacing within children's playgrounds. *ASCE-ASME Journal of Risk and Uncertainty in Engineering Systems, Part B Mechanical Engineering* 2019; 5(1).

38. Eager D, Hayati H and Chapman C. Impulse force as an additional safety criterion for improving the injury prevention performance of impact attenuation surfaces in children's playgrounds. In *ASME 2016 International Mechanical Engineering Congress and Exposition*. American Society of Mechanical Engineers, pp. V014T14A030–V014T14A030.

39. As 4422 playground surfacing-specifications, requirements and test method, 2016.

40. Jayes A and Alexander RM. Estimates of mechanical stresses in leg muscles of galloping greyhounds (canis familiaris. *Journal of Zoology* 1982; 198(3): 315–328.

41. Farley CT, Glasheen J and McMahon TA. Running springs: speed and animal size. *Journal of experimental Biology* 1993; 185(1): 71–86.

Figures

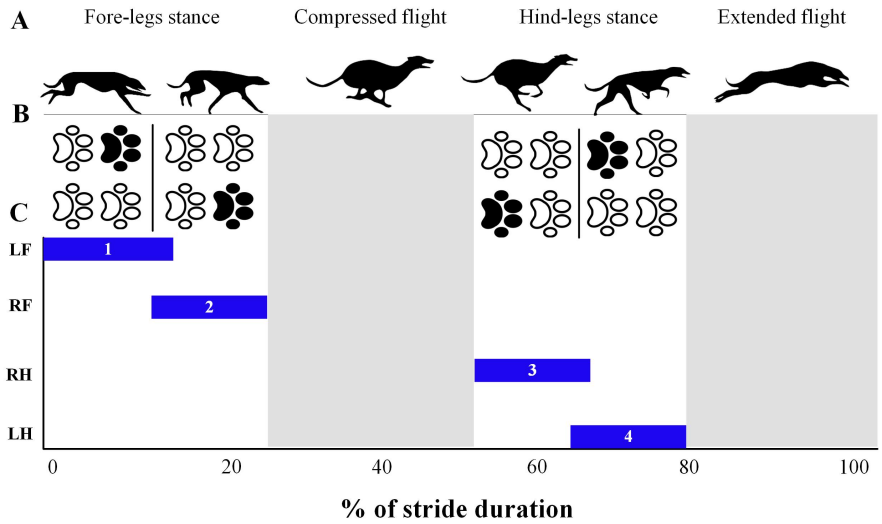

Figure 1. One stride of a galloping greyhound and its corresponding phases. (B) Paw impact pattern of a rotatory gallop. (C) Footfall timing of stride duration in percentages; LF, RF, CFL, RH, LH and EFL stands for left fore-leg, right fore-leg, compressed flight, right hind-leg, left hind-leg and extended flight, respectively.

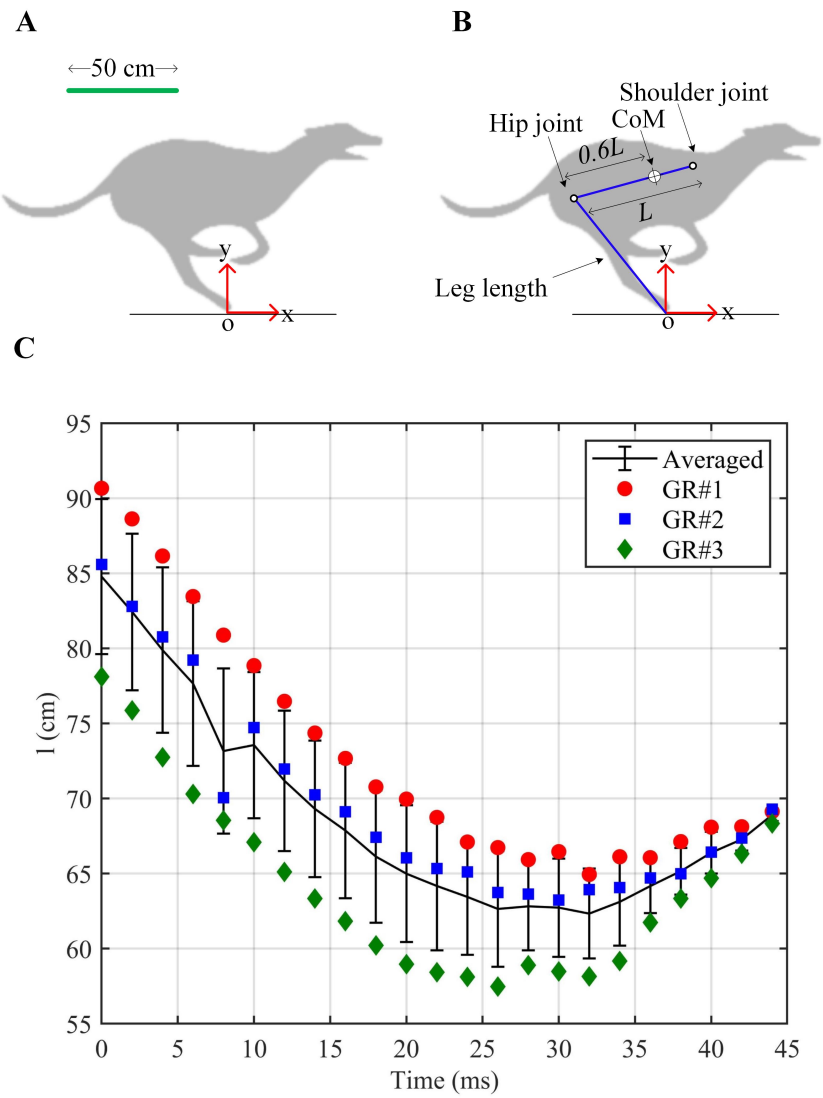

Figure 2. Motion tracking procedure during RH single-support. (A) The coordinate reference point of the system is the touchdown of RH. (B) A reference line from the approximate location of the hip joint and shoulder joint is drawn. The CoM location (60% along the way from hip to shoulder joints) on the reference line is estimated. (C) Greyhounds' hip joint and CoM's dynamics during RH single-support using Kinovea semi-automatic tracking toolbox were tracked. Only the hip joint fluctuation versus time for three data sets are presented here.

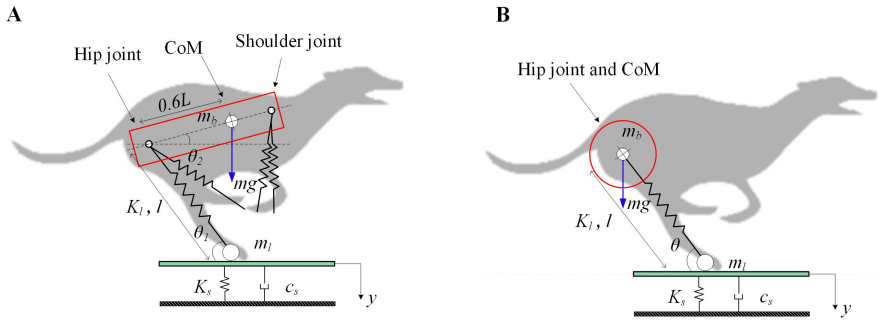

Figure 3. SLIP models of RH single-support of a galloping greyhound. (A) 4 DOF system. (B) 3 DOF system.

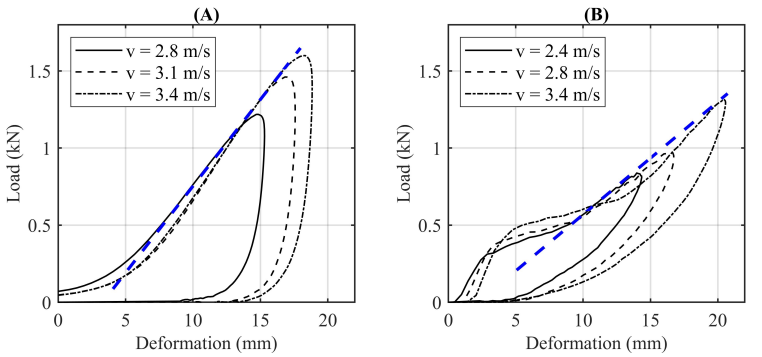

Figure 4. Load-deformation cycles for natural grass for impact velocities of 2.8 to 3.4 m/s (A). Load-deformation cycles for synthetic rubber terrain for impact velocities of 2.4 to 3.4 m/s (B). The slope of the blue dashed line is the effective spring coefficient of surfaces (107 kN/m for natural grass surface and 68.2 kN/m for synthetic rubber surface).

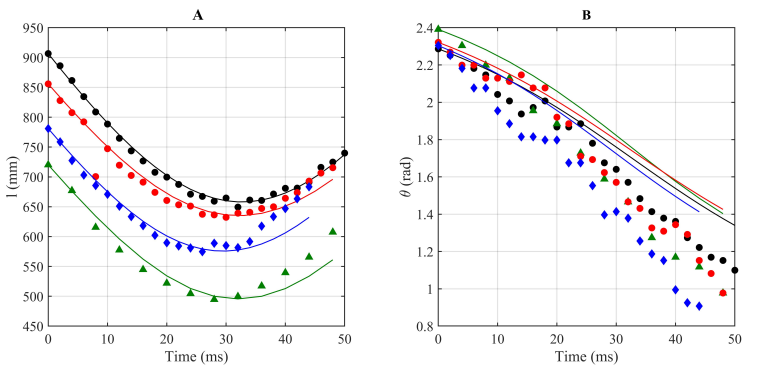

Figure 5. Hind-leg compression vs time (A) and Hind-leg rotation vs time (B) of four greyhounds galloping on the natural grass surface compared with the simulation results. The experimental data and the model results are shown with scattered dots and rigid lines, respectively. The same colours in the scattered plots correspond to the model with similar initial conditions. The root mean square method for the hind-leg compression and leg rotation equalled to 1.59 mm and 0.23 rad, respectively.

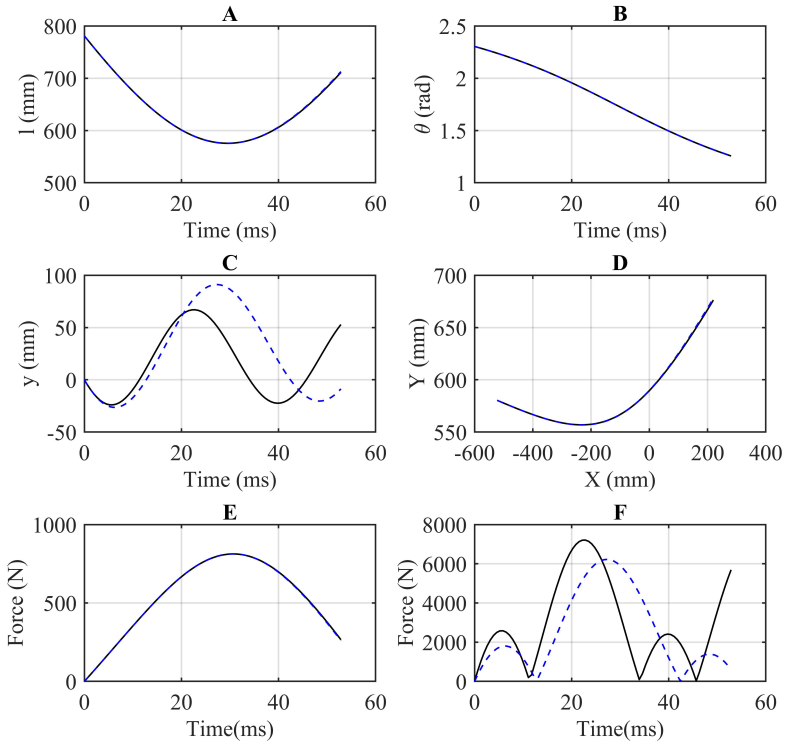

Figure 6. Dynamics of greyhound's RH single-support. Hind-leg compression (A), hind-leg rotation (B), surface compression (C), CoM trajectories (D), Force acting on the CoM (E) and Force acting on the hind-leg (F) on two different surface compliance. The black rigid line represents the natural grass surface and the blue dashed line represents the synthetic rubber surface, respectively.